



Eidgenössische Technische Hochschule Zürich
Swiss Federal Institute of Technology Zurich



Semester Thesis
at the Department of Information Technology
and Electrical Engineering

Sense The Air You Breathe!

Balz Maag

Advisors: David Hasenfratz, Christoph Walser
Professor: Prof. Dr. Lothar Thiele

December 20, 2013

Abstract

Urban air pollution is an ongoing concern in our modern society, since pollutants are harmful to human health and the environment. Therefore it is of high importance to monitor air pollution, which is nowadays usually carried out by static measurement stations. However air pollution is highly location dependent and therefore spatially high-resolved pollution maps are needed. One approach to create such maps is to attach multiple sensor nodes on top of public transportation vehicles, like trams, which are able to cover large urban areas. Due to space and cost limitations these sensor nodes are equipped with small low-cost gas sensors, which are in general applied in industrial setups. Therefore recent sensor solutions weren't able to provide accurate and reliable data for developing precise pollution maps.

In this project a new type of gas sensor is integrated into an existing monitoring solution. On the hardware side, the sensors are embedded into a mobile sensor box with emphasis on providing it with a high-accurate and low-noise power supply, namely a low-dropout voltage regulator, and precise analog to digital sensor signal conversion. On the software side it is shown how the sensor data can be collected by using the backlog interface to transfer data to the back-end server running the Global Sensor Network (GSN).

An elaborate evaluation for carbon monoxide (CO) and nitrogen dioxide (NO_2) sensors show that it is possible to achieve a good performance in comparison to a high accurate measurement station using a simple calibration technique. However, the evaluation also points out that such low-cost gas sensors are sensitive to interfering gases, in this case the NO_2 sensor is highly sensitive to ozone (O_3), which can not be avoided in an urban environment and therefore illustrates the limitations of such sensors up to date.

Acknowledgement

I would like to thank my supervisors David Hasenfratz and Christoph Walser for their never-ending support during this project and Prof. Lothar Thiele and the Computer Engineering and Networks Laboratory TIK for providing the facilities and equipment. Special thanks also go the "Nationales Beobachtungsnetz für Luftfremdstoffe (NABEL)" for helping us testing our sensors at the NABEL measurement station in Dübendorf.

Contents

Abstract	i
1. Introduction	1
1.1. Urban Air Pollution	1
1.2. The Opensense Project	1
1.3. Integrating Electrochemical Gas Sensors	3
2. Hardware	5
2.1. System Overview	5
2.2. Alphasense B4 Gas Sensors	6
2.3. Power Supply	7
2.4. Analog-Digital Conversion	9
2.5. Final Design	11
3. Software	17
3.1. System Overview	17
3.2. The Backlog Interface	17
3.3. GSN	20
4. Evaluation	25
4.1. NABEL Reference Station	25
4.2. Overall Results	34
Conclusions and Future Work	35
Bibliography	37
A. Appendix	39
A.1. Hardware	40
A.2. Software	45
List of Tables	47
List of Figures	49

1

Introduction

1.1. Urban Air Pollution

Urban air pollution is a major concern in modern society, especially in large cities. Vehicular traffic and combustion-based power generation in industry are the most significant sources of different air pollutants, which have considerable effects on human health and the environment. The most important gases which are considered as primary pollutants and therefore frequently monitored are carbon monoxide (CO), nitrogen oxides (NO and NO_2), ozone (O_3), sulfur dioxide (SO_2) and hydrogen sulfide (H_2S). They have a strong influence on illnesses like asthma, lung cancer and migraine but also on environmental issues like acid rain and ozone layer depletion. Due to these impacts, urban air pollution monitoring has become an important matter.

1.2. The Opensense Project

Nowadays, air pollution monitoring is usually carried out by static measurement stations, which are operated by official authorities, e.g. the "Nationales Beobachtungsnetz für Luftfremdstoffe (NABEL)" [14] in Switzerland. In general, these stations are able to measure a large variety of pollutants in a highly reliable and accurate manner. On the other hand, their acquisition and operation is expensive and therefore allows

only a limited number of installations. Consequently a disadvantage of these static monitoring networks is their inability to gather detailed information about the spatial distribution of air pollutants. However, urban air pollution is in general highly location dependent, e.g. the concentrations are higher in industrial areas or along highly frequented roads, which is shown in Fig. 1.1. The concentration of ultrafine particles in Zürich is notably higher along roads with high traffic densities and in urban agglomerations compared to rural areas. This spatial variability

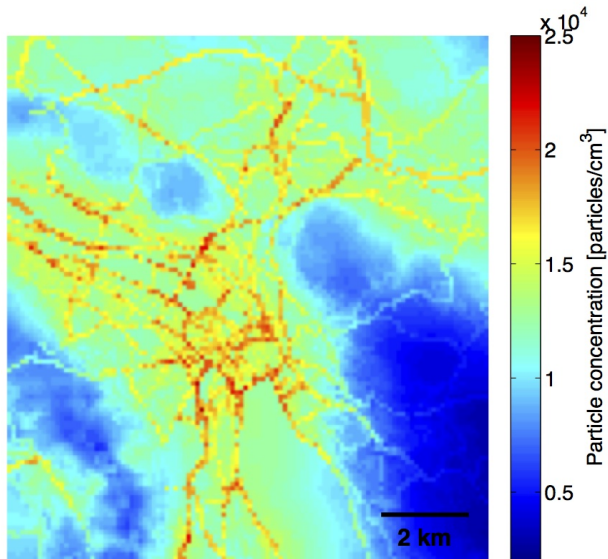


Fig. 1.1.: Ultrafine particle distribution in Zürich in the fall of 2013 [10]

emphasizes the need of highly resolved pollution maps, like the one in Fig. 1.1. To meet this challenge the OpenSense Project at ETH Zürich [10] uses multiple mobile sensor nodes, which are installed on top of trams of the public transport network. Due to Zürich's well-developed and extensive tram network it is possible to sense pollutants in an area of 100 km^2 .

Currently 10 trams of the "Verkehrsbetriebe Zürich (VBZ)" are equipped with measurement stations, like the one shown in Fig. 1.2, and gather sensor readings during several hours every day on different routes in the city area.



Fig. 1.2.: Sensor box on a VBZ Cobra-tram [10]

1.3. Integrating Electrochemical Gas Sensors

1.3.1. Existing Solution

The sensor boxes are equipped with low-cost gas sensors. Currently every box is armed with a subset of four different sensors to monitor airborne pollutants:

- Ozone (O_3): *MiCS-OZ-47, Ozone Sensing Head with Smart Transmitter PCB* by SGX Sensortech [11]
- Carbon monoxide (CO): *CO-AF Carbon Monoxide Sensor* by Alphasense [4]
- Nitrogen dioxide (NO_2): *NO2-A1 Nitrogen Dioxide Sensor* by Alphasense [6]
- Ultrafine particle (UFP): *MiniDiSC* by Matter Aerosol [1]

The CO and NO_2 sensors are interfaced through a *Digital Transmitter Board* from Alphasense [2], which takes care of the power supply and analog to digital signal conversion. However, the performance of the sensors in combination with the digital transmitter board is not satisfying. The resulting outputs are inaccurate and show significant noise, which makes the measurements unusable. The underlying problems are twofold. On the one hand low-cost gas sensors are usually optimized for industrial purposes, which means they are designed to measure larger gas concentrations than what is found in ambient air and have stable environmental conditions (e.g. temperature and humidity). On the other hand the power supply and AD-conversion on the transmitter board are not implemented in an optimal manner.

1.3.2. New Solution and Road Map

Alphasense has recently launched a new type of electrochemical gas sensors, the B4 series, which is designed to monitor air quality in ambient air, i.e. the resolution of the gas sensors is in the low ppb-range. In this project two of these new sensors, the CO-B4 [5] and the NO₂-B4 [7] are integrated in the current setup of OpenSense with emphasis on an optimal power-supply and AD-conversion. The hardware solution from Alphasense is renounced and a custom-built PCB is used, which takes care of voltage regulation and the conversion of analog sensor signals to digital values.

The remainder of this report is structured as follows:

In Chapter 2 the Alphasense B4 gas sensors are introduced and an improved hardware solution is presented by motivating the need of an accurate and low-noise power supply and a precise AD-conversion.

Chapter 3 describes how the sensor data is read and processed in the backlog software of the OpenSense system and in a second stage how it is transferred to the back-end server running the Global Sensor Network (GSN) [13]: A middleware for fast and flexible sensor network deployment.

The work concludes in Chapter 4 with the evaluation of the sensor performance by comparing the low-cost sensor measurements to sensor data from an accurate and reliable static measurement station.

2

Hardware

2.1. System Overview

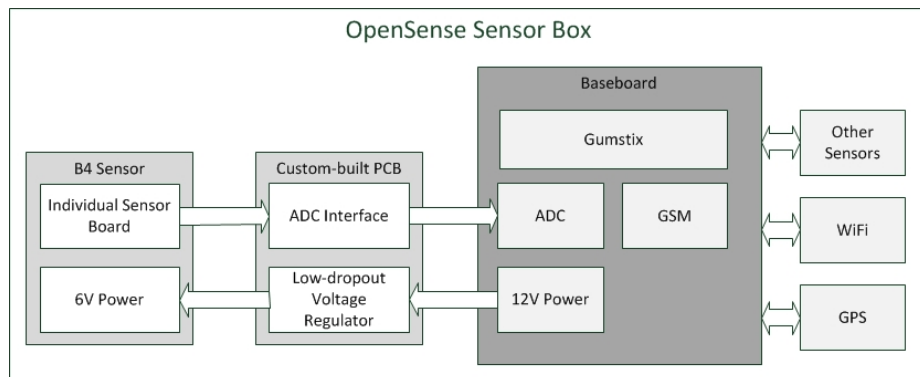


Fig. 2.1.: Coarse overview of hardware components

The heart of each sensor box is a baseboard, which contains a Gumstix, a computer-on-module that runs an embedded Linux OS. For communication it is equipped with WiFi and GSM modems. A GPS module keeps track of the sensor node's location. The sensor node is equipped with different sensors like O_3 , ultrafine particle, humidity and temperature. A DC-DC converter regulates 24 V provided by the tram down to 12 V to power the whole board. Further, an analog-to-digital converter (ADC) can read up to 10 input channels.

The B4 sensor requires a 6 V power supply, which is generated by a voltage regulator and the sensor signals are converted by the baseboard's ADC

to digital values. Further details on these components are presented in this chapter.

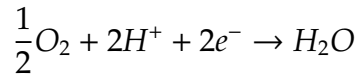
2.2. Alphasense B4 Gas Sensors

2.2.1. Physical background

Alphasense B4 toxic gas sensors are based on electrochemical cells [3]. When gas diffuses through the sensor it is either oxidized (CO, H_2S, NO) or reduced (O_3, NO_2) at a working electrode (WE). This electrochemical reaction generates a current, which is proportional to the concentration in the air. For example the reaction at the working electrode for CO is



A second electrode, called counter electrode, balances the overall reaction by reducing oxygen using H^+ and the electrons from the working electrode:



The current induced by the electrons flowing between the two electrodes is linearly proportional to the CO concentration and can be measured using a load resistor between them.

B4 sensors use two additional electrodes: a reference and an auxiliary electrode (AUX).

The function of the AUX electrode is similar to the WE, but the electrode itself does not come in contact with the target gas. It measures the influence of the environmental conditions, which can be used for zero current drift compensation.

The reference electrode is stabilizing the sensing electrodes' (WE and AUX) electrochemical potentials, which generates an offset voltage in their sensing signals.

2.2.2. Individual Sensor Board (ISB)

Each sensor has an individual sensor board, which contains an operational amplifier that is providing balance current to the counter electrode. Further the working and auxiliary electrodes are equipped with equivalent two stage amplifiers, which transfer the sensor current into voltage.

Every sensor is shipped with an ISB and they have their individual offset voltages (WE and AUX), which are marked on the package. Therefore the sensor and its specific ISB must always be used in combination.

2.3. Power Supply

The ISB requires a 6 ± 0.2 V DC power supply, which should be to achieve best results low-noise and decoupled. Because the baseboard contains no 6 V supply but only 3.3 V, 4.2 V, 5 V and 12 V DC levels, a voltage conversion needs to be done. There are three possible solutions:

1. *DC-DC boost converter*: A low input voltage (3.3 V, 4.5 V, 5 V) is increased to the required 6 V output level.
2. *DC-DC buck converter*: A high input voltage (12 V) is decreased to the required 6 V output level.
3. *Low-dropout linear voltage regulator (LDO)*: Same concept as point 2, but different approach.

The basic operation principle of DC-DC boost/buck converters is the periodical storage of energy in an inductor. By varying the time during the energy is stored and low-pass filtering the output voltage, the input voltage can be regulated to a different output level. The advantage of this concept is its energy efficiency. A drawback, however, is the output noise due to the fast switching and possibly remaining oscillations, which cannot be filtered out.

The basic concept of an LDO is a voltage divider network in which the output voltage is always held constant. The most important advantage compared to DC-DC converters is that LDOs show in general less output noise, because there is no fast switching involved. A drawback is its low energy efficiency, because the difference between the input and output voltage is lost as waste heat, which can be problematic if the load at the output draws high currents.

Based on these facts and because the energy consumption of the sensors is very small (around a few μ A) and the power supply should produce as less noise as possible, an LDO was chosen to be used.

2.3.1. Low-Dropout Voltage Regulator LF60AB

The two main-criteria for the appropriate choice of an LDO in order to fit the requirements are:

- **Accuracy:** An LDO usually has an offset from the designated output voltage, which is different for each component. The range of this offset is specified by the manufacturer and should be as small as possible.

- **Output noise:** The amplitude and spectrum of the noise in the output voltage during operation with a non-zero load should also be as small as possible.

Considering these criteria, the choice fell to the model *LF60AB* by STMicroelectronics [12], whose specifications are shown in Table 2.1.

Parameter	Minimum	Typical	Maximum
Output voltage V_O	5.88 V	6 V	6.12 V
Input voltage V_I	6 V	n/a	16 V
Output noise amplitude	n/a	$50\mu\text{V}$	n/a
Output noise spectrum	10Hz	n/a	100kHz

Tab. 2.1.: LF60AB specifications

This model outperforms many other similar LDOs, for example the *uA78M06* by Texas Instruments [9], which has an offset in a range of [5.7 V, 6.3 V] and has in the same spectrum a maximum noise of $200\mu\text{V}$.

2.3.2. Decoupling Circuit

The LDO's input must be decoupled from its power supply, which can be done by using a capacitor between input (IN) and ground (GND). This circuit then filters out high-frequency ripples, which may be produced by the external supply or picked up by wires and connections. The same needs to be done at the LDO's output side (OUT). The resulting circuit is shown in Fig. 2.2. The sizes, $0.1\mu\text{F}$ at the input and $2.2\mu\text{F}$ at the output, are recommended by STMicroelectronics.

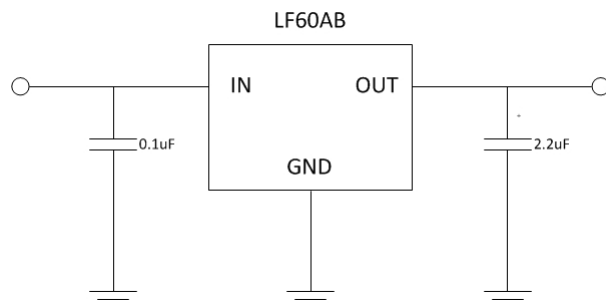


Fig. 2.2.: LDO with decoupling capacitors

2.4. Analog-Digital Conversion

The choice of an appropriate ADC is based on the sensor and ISB specifications. Table 2.2 illustrates the important parameters for all available B4 sensor types.

Parameter	H_2S	CO	NO	NO_2	SO_2	O_3
Resolution R_s [ppb]	4	10	5	5	3	3
Min. Sensitivity S_{min} [mV/ppb]	1.6	0.23	0.55	0.34	0.37	1
Max. Sensitivity S_{max} [mV/ppb]	1.7	0.45	0.94	0.52	0.52	1.2
Min. Resolution output $R_{out,min}$ [mV]	6.4	2.3	2.75	1.7	1.11	3
Max. Resolution output $R_{out,max}$ [mV]	6.8	4.5	4.65	2.6	2.56	3.6
WE zero offset Off_{WE} [mV]	350	270	545	225	355	260
Full scale F [ppm]	3	13	6	11	11	5
Max. Output Out_{max} [V]	5.45	6.12	6.125	5.945	6.075	6.26

Tab. 2.2.: Sensor and ISB specifications

Comments on Table 2.2:

- *Resolution* [ppb] denotes the smallest possible gas concentration a sensor can distinguish.
- *Sensitivity* [mV/ppb] shows the change in output voltage per ppb concentration change. This value lies typically in a range between the given minimum and maximum values.
- *Minimum/maximum resolution output* [mV]

$$R_{out,min} = R_s \cdot S_{min} \quad R_{out,max} = R_s \cdot S_{max}$$

which is the smallest change in the output voltage. This is of high importance, because the ADC needs to be able to measure the smallest change among all sensors.

- *WE zero offset* [mV] is the output voltage in clean air. This is only a typical value, the true value is marked for each sensor/ISB pair on the packaging.
- *Full scale* [ppm] is the highest gas concentration a sensor can measure.
- *Maximum Output* [mV]

$$Out_{max} = Off_{WE} + S_{max} \cdot F$$

which is the maximal voltage a sensor can produce if it measures its full scale concentration.

The baseboard ADC is an *AD7708* by Analog Devices [8] with the specifications given in Table 2.3.

Parameter	Value
Resolution	16Bit
Input range	$20mV - 2.56V$
Channels	10

Tab. 2.3.: AD7708 specifications

Comments on Table 2.3:

- A 16Bit resolution is equal to a $2^{16} = 65536$ LSB representation.
- With the given input range the sensitivity equals to

$$\frac{2.56 V - 0.02 V}{65536} = 38.8 \frac{\mu V}{LSB}$$

This value is small enough to measure the smallest minimum output resolution $R_{out,min}$ in Table 2.2, which is $1.11 mV$ for the SO_2 sensor.

Because the AD7708 can only measure up to $2.56 V$, but the maximal possible output is $6.26 V$ (Table 2.2: Out_{max} for O_3), the sensor signal levels need to be shifted. This can be done by using a voltage divider, which only requires two resistors as shown in Fig. 2.3.

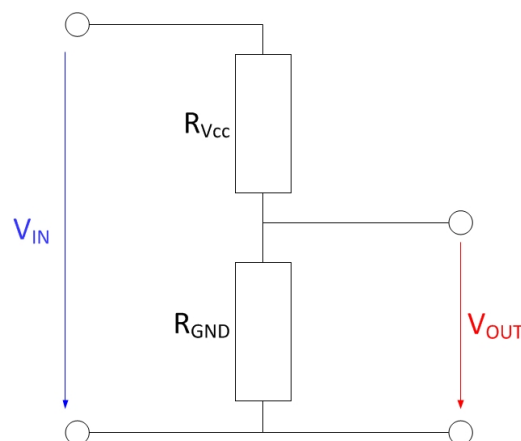


Fig. 2.3.: Voltage divider circuit

The relation between V_{IN} and V_{OUT} is given by

$$V_{OUT} = V_{IN} \cdot \frac{R_{GND}}{R_{Vcc} + R_{GND}}$$

With setting $V_{OUT} = 2.5V$ and $V_{IN} = 6.26 V$ we get:

$$\frac{V_{OUT}}{V_{IN}} = 0.399 \approx \frac{66.5 k\Omega}{100 k\Omega + 66.5 k\Omega}$$

Therefore, a suitable voltage divider setup is given by $R_{GND} = 66.5 k\Omega$ and $R_{Vcc} = 100 k\Omega$.

By applying this voltage divider, all the values in Table 2.2, except R_S and F , need to be multiplied by $\frac{66.5 k\Omega}{100 k\Omega + 66.5 k\Omega} \approx 0.399$. The most important ones can be seen in Table 2.4.

Parameter	H_2S	CO	NO	NO_2	SO_2	O_3
S_{max} [mV/ppb]	0.678	0.180	0.375	0.207	0.207	0.479
$R_{out,min}$ [mV]	2.505	0.918	1.097	0.678	0.443	1.197
Off_{WE} [mV]	139.7	107.7	217.5	89.8	141.6	103.7
Out_{max} [V]	2.175	2.442	2.444	2.372	2.424	2.5

Tab. 2.4.: Sensor/ISB specifications after voltage level shift by factor 0.399

The smallest minimum output resolution which needs to be measured is now equal to $1.11 mV \cdot 0.399 = 0.443 mV$. This value is still larger than the ADC's resolution of $38.8 \mu V$ and therefore it is still possible to measure the resolution of the SO_2 sensor. All the other values are noncritical.

This analysis shows that the baseboard ADC is an appropriate choice for accurately converting the analog sensor signals to digital values without loosing any information.

2.5. Final Design

2.5.1. Printed Circuit Board

The LDO (see Chapter 2.3) and the interface to the ADC (see Chapter 2.4) are combined on a PCB, which can be mounted to the ISB.

Schematics

The schematics contain four parts:

1. *Decoupled LF60AB, Fig. 2.4:* The LF60AB is regulating the 12V (VCC_12) input to 6V (VCC_6) output voltage. The two capacitors ($0.1\mu F$ ceramic and $2.2\mu F$ tantalum) decouple both voltages.

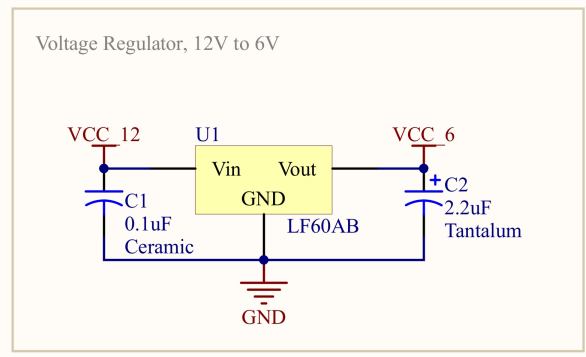


Fig. 2.4.: Decoupled LF60AB circuit

2. *Voltage dividers, Fig. 2.5:* OP1+ corresponds to the working electrode and OP2+ to the auxiliary electrode. To interface the baseboard R3 and R4 have a $200\text{ k}\Omega$ resistance, because on the baseboard the ADC input is connected to a $100\text{ k}\Omega$ pull down resistor. These two parallel resistors connect each ADC channel to GND with a resistance of

$$R_{tot} = \left(\frac{1}{100\text{ k}\Omega} + \frac{1}{200\text{ k}\Omega} \right)^{-1} = 66.6\text{ k}\Omega$$

Therefore, in total this corresponds to the solution proposed in Chapter 2.4.

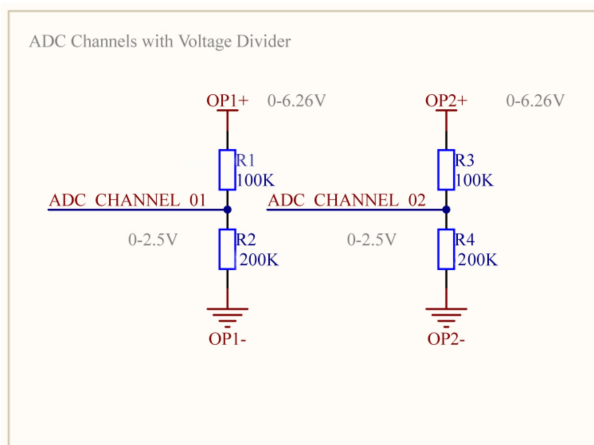


Fig. 2.5.: Voltage divider circuits and ADC channel inputs

3. *ISB connector, Fig. 2.6:* A 6x1 pin socket connects the PCB to the ISB. Pin 1 and 2 power the sensor with 6 V. Pin 3/4 and 5/6 are the WE and AUX signals.

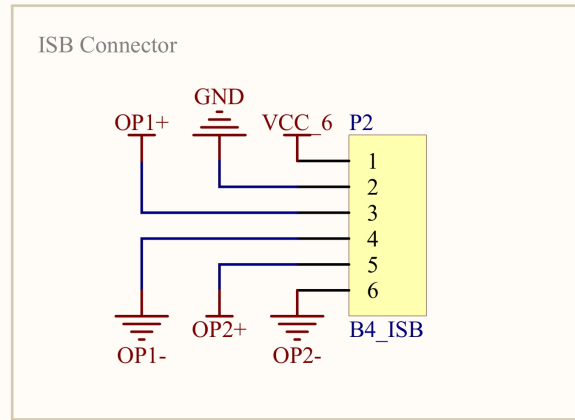


Fig. 2.6.: ISB Connector

4. *Power input and ADC channels, Fig. 2.7:* A 6x1 header takes the 12 V voltage input from the baseboard and accesses the voltage dividers.

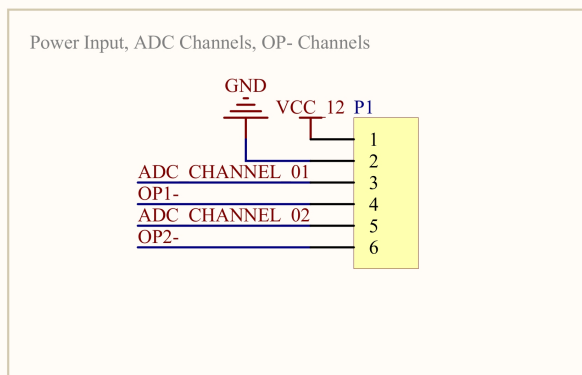


Fig. 2.7.: Power input and ADC channels

Layout

Fig. 2.8 shows the top layer of the PCB layout. It has the same diameter and holes as the ISB, so they can be stacked.

The PCB mounted to the ISB and its corresponding sensor is shown in Fig. 2.9

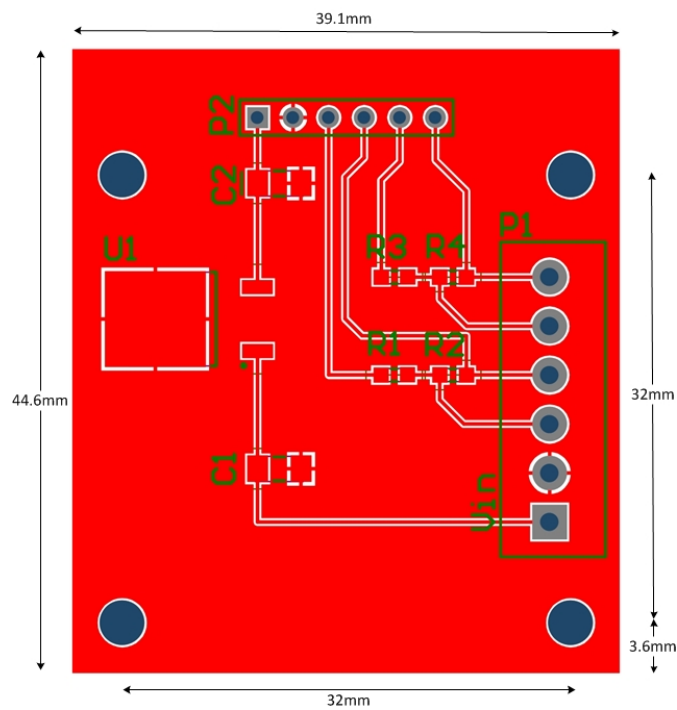


Fig. 2.8.: PCB layout

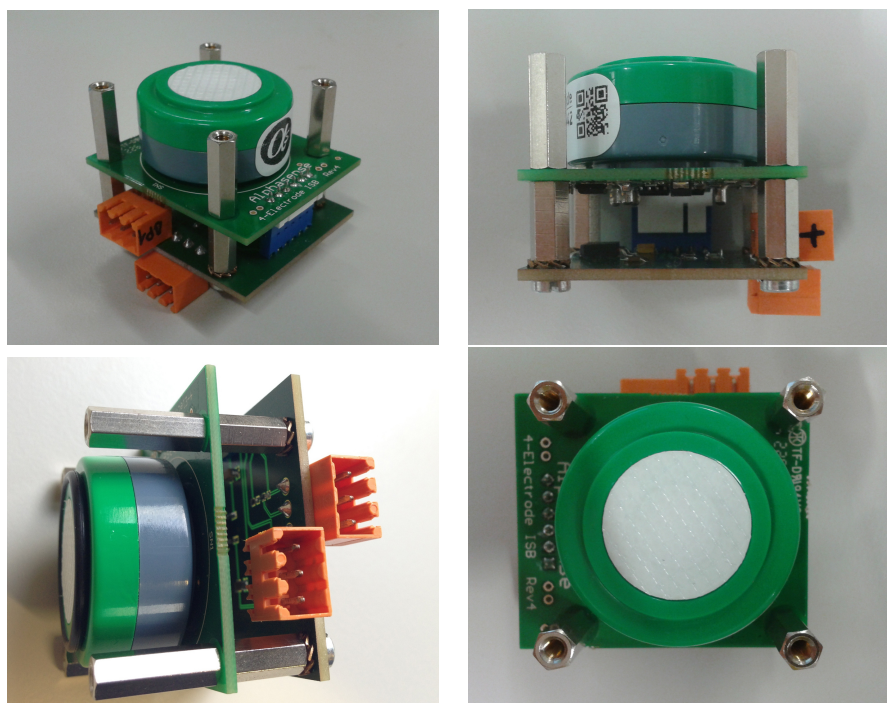


Fig. 2.9.: Stacked PCBs and the B4 sensor head

2.5.2. Integration into the OpenSense Measurement Box

The sensors are screwed from inside the box to the wall. The sensor head is put through a hole and is water protected by a cover, as shown in Fig. 2.10.

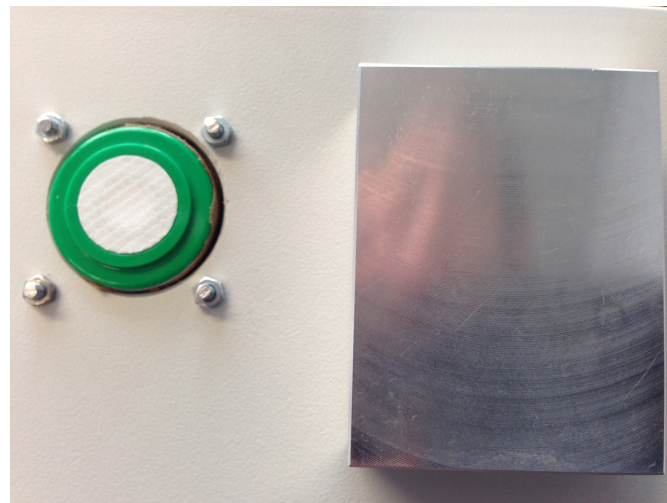


Fig. 2.10.: Exterior wall of the OpenSense measurement box, left: B4 sensor head, right: sensor cover

The final box, which will be used to analyze the performance of the sensors is shown in Fig. 2.11. It is equipped with two B4 sensors to measure CO and NO₂ concentrations.

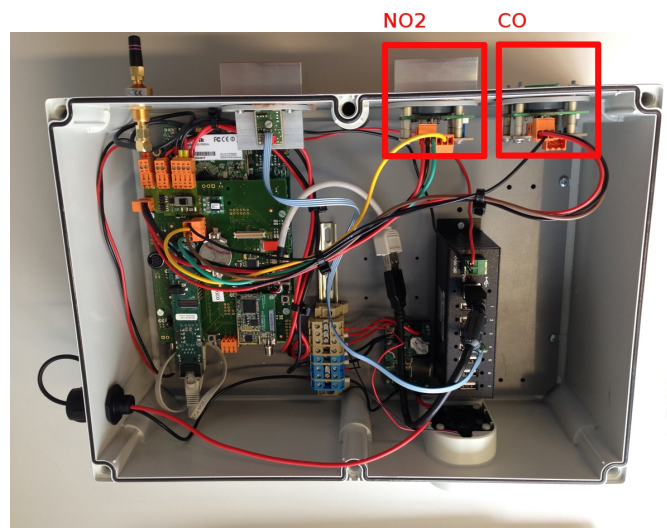


Fig. 2.11.: OpenSense measurement box with two B4 sensors to monitor CO and NO₂ concentrations

2.5.3. Faraday Cage

The gas sensors and associated electronics are susceptible to electromagnetic pickup. Therefore, the sensors should ideally be placed inside a Faraday cage. A Faraday cage is a container made out of conducting material, e.g. copper mesh.

To work properly, the whole spectrum of electromagnetic waves, which occur in an urban environment must be blocked. The waves can be blocked if the mesh width is at most half the corresponding wavelength λ . Assume that the largest considerable frequency is 5 GHz generated by WiFi access points. Therefore it follows for the mesh width w :

$$w < \frac{\lambda}{2} = \frac{\frac{300000 \text{ km/s}}{5 \text{ GHz}}}{2} = 3 \text{ cm}$$

This is of course only a theoretical result, in practice a mesh width smaller than 3 cm should be chosen. To provide a complete blocking all the connecting wires need to be shielded as well.

The design and mounting of such a Faraday cage needs further investigations, e.g. construction and testing, which exceed the possibilities of this project and therefore a Faraday cage was not implemented.

3

Software

3.1. System Overview

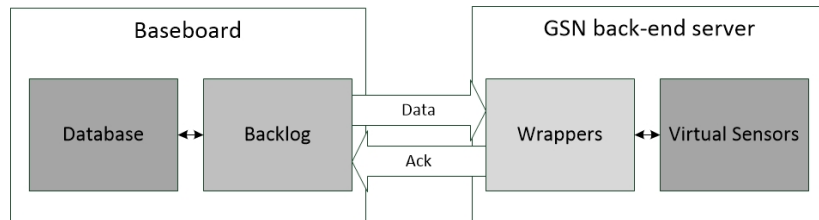


Fig. 3.1.: Coarse overview of the different software parts

Fig. 3.1 shows a coarse overview of the most important software parts. The system can be partitioned in two individual blocks:

- On the baseboard side a backlog software acquires sensor data and stores them in a first step in a local database.
- A back-end server, running the *Global Sensor Network* (GSN) [13] is used to collect and process the data from all the sensor nodes.

More details on these two blocks are described in this chapter.

3.2. The Backlog Interface

A python interface called *backlog* manages all the different tasks of the sensor box, e.g. sensor readings, GPS data acquisition and database

operations. It contains different plugins, one for each individual task, for example the GPS plugin periodically reads data from the GPS device. Some plugins may need a further driver between the hardware and software. In our case, in order to read and store the sensor signals, a new plugin with a driver is integrated into the backlog system.

3.2.1. B4 Sensor Driver

The kernel module for the ADC called *ad77x8.ko* is reading out the ADC channels and periodically writing their values into a virtual file, one for each channel. The file is based on a special unix-filesystem called *procfs*, it is specialised for accessing process data in the kernel space. Further it is possible to write the configuration of the ADC.

Therefore to get the sensor data it is sufficient to simply read the proc files, this is done in the B4 sensor driver (*B4SensorDriver.py*). For each channel which needs to be read, an object of the class *B4SensorDriver* has to be created. The class itself implements two public functions:

- *_read(self)*: This function reads the proc file according to the channel (1, 2 or 3). It returns the value in [mV].
- *_adc_config(self)*: Writes the configuration file for the ADC. Different parameters can be parsed as listed in Table 3.1.

Parameter	Description	Default
<i>format</i>	Output format: raw (raw) register values or voltage (mV)	mV
<i>chopping</i>	ADC optimization [on/off]	on
<i>negbuf</i>	Buffered input [on/off]	on
<i>sf</i>	Conversion rate [13-255]	13
<i>range</i>	ADC input range [0-7]	7
<i>calibrate</i>	Calibration for all channels [on/off]	off

Tab. 3.1.: ADC configuration options

In general the default values are the preferred setting and therefore *_adc_config* is not needed.

3.2.2. B4 Sensor Plugin

The *B4SensorPlugin.py* is responsible for reading and processing the sensor data. Its basic workflow is shown in Fig. 3.2.

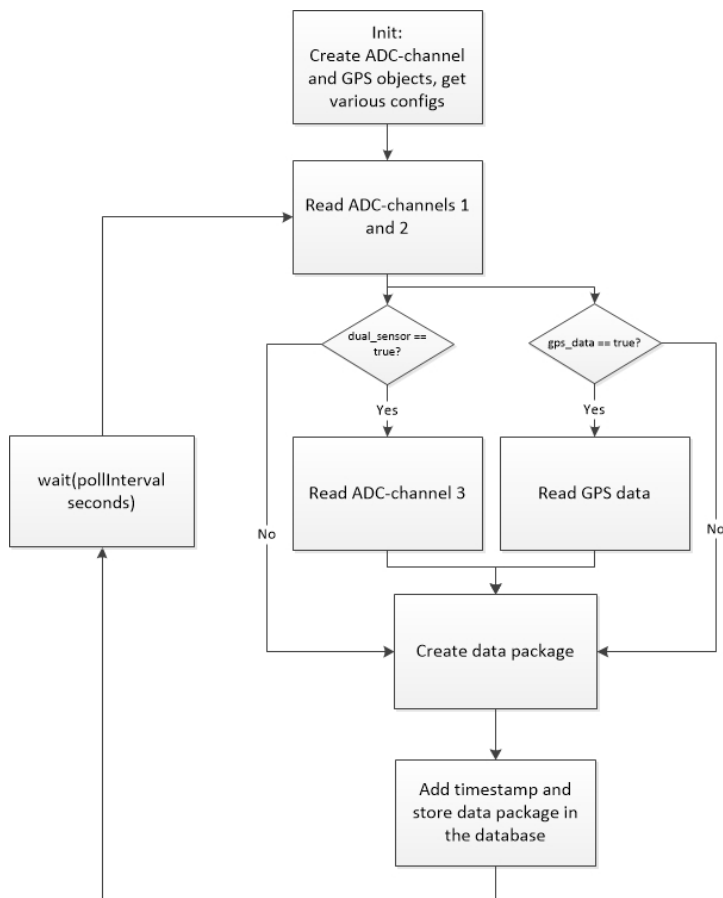


Fig. 3.2.: B4 plugin basic flowchart

During the initialization phase objects for the ADC channels and the GPS device are created and important configurations imported, e.g. proc-file locations. After this different actions are carried out:

- ADC-channels 1 and 2 are always read, these correspond to the working and auxiliary electrode of one sensor, respectively. Because the data from channel 1 is proportional to the target's gas concentration, it is also converted from *mV* to *ppm*. The conversion is done according to the following equation:

$$\text{Value[ppm]} = \frac{\text{Value[mV]} - \text{WE Offset[mV]} \cdot \text{Shift Ratio}}{\text{Sensitivity[nA/ppm]} \cdot \text{ISB Gain[mV/nA]} \cdot \text{Shift Ratio}}$$

- If a second sensor is installed, ADC channel 3 has to be read out as well. This channel corresponds to the working electrode and is also converted to *ppm*.
- It is optional to read also the GPS device.
- All gathered data is combined to a data package, which can have different formats according to what optional data is available.
- The data package gets a timestamp and is stored in the local database.
- The plugin puts itself to a sleeping mode for a predefined time, after this the whole process starts over. The default sleeping time is 10 sec

3.3. GSN

To collect all the data the sensor boxes communicate with a back-end server. This server is running the *Global Sensor Network* (GSN), a middleware which manages data collection in sensor networks. The main purpose is to provide a infrastructure for a sensor network, which consists of multiple heterogeneous sensor nodes. GSN abstracts from specific sensor data to a data stream, in general the data is streamed into the system through multiple *wrappers* and then processed by *virtual sensors*. In other words the wrapper's job is to acquisit data from any specific type of device and provide it to a virtual sensor which will process (e.g. combine it with other data) and store it in the GSN database.

In order to integrate the B4 sensor into the OpenSense GSN, a wrapper which gathers the data from the backlog database and a description of the virtual sensor must be provided, this chapter presents how this is done.

3.3.1. B4 Sensor Wrapper

The B4 sensor wrapper, implemented in *B4SensorPlugin.java*, makes sure that GSN receives the data coming from the baseboard. It requests B4SensorPlugin packages (through backlog message identifier 115) and encapsulates the data into the standard GSN data model. The most important part is that the wrapper differs between all the possible formats of the received data package, which has been created on the backlog side. This can be done by counting the number of elements in the package and mainly depends on the number of employed sensors and if data from the GPS device is included. The possibilities are shown in Table 3.2.

Data Length	Data Fields
3	ADC channel 1 [mV] ADC channel 1 [ppm] ADC channel 2 [mV]
5	ADC channel 1 [mV] ADC channel 1 [ppm] ADC channel 2 [mV] ADC channel 3 [mV] ADC channel 3 [ppm]
17	14 GPS data fields ADC channel 1 [mV] ADC channel 1 [ppm] ADC channel 2 [mV]
19	14 GPS data fields ADC channel 1 [mV] ADC channel 1 [ppm] ADC channel 2 [mV] ADC channel 3 [mV] ADC channel 3 [ppm]

Tab. 3.2.: Different data package formats

The wrapper assigns this data to the GSN data model *DataField*, which in our case holds the following elements:

```
private DataField[] dataField = {
    new DataField("TIMESTAMP", "BIGINT"),
    new DataField("GENERATION_TIME", "BIGINT"),
    new DataField("DEVICE_ID", "INTEGER"),
    new DataField("UTC_RAW_DATA", "VARCHAR(32)"),
    new DataField("LAT_RAW_DATA", "VARCHAR(32)),
```

```

new DataField("LAT_N_RAW_DATA", "VARCHAR(32)") ,
new DataField("LONG_RAW_DATA", "VARCHAR(32)") ,
new DataField("LONG_N_RAW_DATA", "VARCHAR(32)") ,
new DataField("QUAL_RAW_DATA", "VARCHAR(32)") ,
new DataField("SAT_RAW_DATA", "VARCHAR(32)") ,
new DataField("HDOP_RAW_DATA", "VARCHAR(32)") ,
new DataField("GEO_HEIGHT_RAW_DATA", "VARCHAR(32)") ,
new DataField("GEO_HEIGHT_U_RAW_DATA", "VARCHAR(32)") ,
new DataField("GEO_SEP_RAW_DATA", "VARCHAR(32)") ,
new DataField("GEO_SEP_U_RAW_DATA", "VARCHAR(32)") ,
new DataField("ADC_CHANNEL_01_MV", "DOUBLE") ,
new DataField("ADC_CHANNEL_01_PPM", "DOUBLE") ,
new DataField("ADC_CHANNEL_02_MV", "DOUBLE") ,
new DataField("ADC_CHANNEL_03_MV", "DOUBLE") ,
new DataField("ADC_CHANNEL_03_PPM", "DOUBLE") };
```

The data can now be processed by a virtual sensor, more details on this in the next chapter.

After the wrapper successfully received and assigned a data package, it sends an acknowledgement message to the baseboard, so the data package can be removed from the local database. This prevents the backlog from sending duplicates and packet losses on the GSN side.

3.3.2. Virtual Sensor

The virtual sensor is the main component of the GSN system, it receives data from one or more wrappers, processes and stores it. The structure of the virtual sensor is defined in a *.xml* file. It describes which data fields are stored and which wrappers provide this data. It is also possible to derive a virtual sensor from another one, that is the data is not provided by a wrapper but by another virtual sensor.

In our case there are two virtual sensors:

- *OpenSense_B4Sensor_raw.xml* which stores the raw data from the *B4SensorPlugin.java* wrapper.
- *OpenSense_B4Sensor_mapped.xml* which is based on *OpenSense_B4Sensor_raw.xml*. It parses the data, in particular converts the raw GPS data to a common format and specifies the units (mV and ppm) of the ADC-channel values.

3.3.3. Final Design

Through a web interface the GSN data can be accessed. Fig. 3.3 shows the mapped virtual sensor. The depicted readings were taken on Saturday the 7th December 2013 at 14:21:21 CET, GPS data is turned off and all three channels are read.

ostest_b4sensor__mapped 07/12/2013 14:21:21.986 CET	
Real-Time	Structure
device_id	1
generation_time	07/12/2013 14:21:21.916 CET
timestamp	07/12/2013 14:21:21.916 CET
utc_pos_time	null
latitude	null
lat_hemisphere	null
longitude	null
long_hemisphere	null
quality	null
nr_satellites	null
hdop	null
geoid_height	null
geoid_height_unit	null
geoid_sep	null
geoid_sep_unit	152.656 mV
adc_channel_01_mv	0.17159703266251655 ppm
adc_channel_01_ppm	139.453 mV
adc_channel_02_mv	97.07 mV
adc_channel_03_mv	-0.04726404353456174 ppm
adc_channel_03_ppm	

Fig. 3.3.: Virtual sensor data from 7th December 2013 at 14:21:21.986 CET

The data of each data field can also be plotted over time, which is shown for the CO [ppm] value in Fig. 3.4.

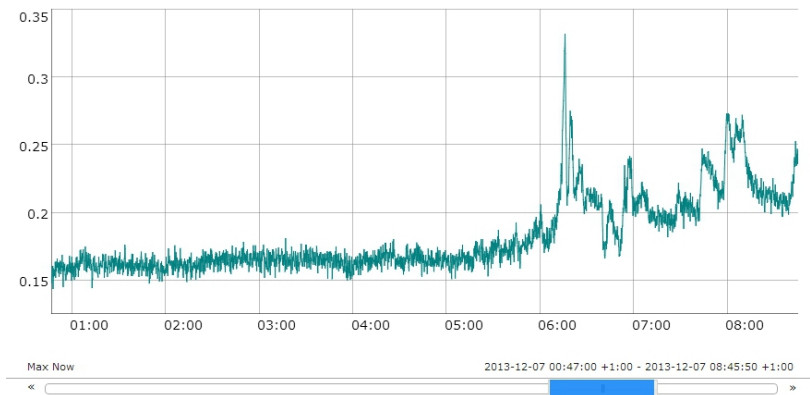


Fig. 3.4.: CO [ppm] data on the 7th December 2013 between 00:47 and 08:45 CET

4

Evaluation

4.1. NABEL Reference Station

In this chapter the measurements of the B4 sensors are compared to a static measurement station in Dübendorf (ZH) operated by the "Nationales Beobachtungsnetz für Luftfremdstoffe (NABEL)". The measurement station monitors various pollutants including carbon monoxide (CO) and nitrogen dioxide (NO_2). The readings of these two sensors will not only be used to review our setup but also to derive a calibration for the B4 sensors.

The OpenSense measurement box was been placed on top of the NABEL measurement station building, which is shown in Fig. 4.1.

4.1.1. Carbon Monoxide

Between 3rd December 2013 14:40:00 CET and 7th December 2013 08:00:00 CET the sensor box collected CO data, which is shown with the according NABEL readings in Fig. 4.2.

Because NABEL only provides average data values over a period of 10 minutes, the B4 values have been aggregated as well over 10 minutes.

Raw data

The plot in 4.2 shows an offset, which is maximal for high CO concentrations ($> 0.3 \text{ ppm}$) and decreases for lower concentrations. The absolute offset lies in the range of $[10^{-4}, 0.38] \text{ ppm}$ with an average absolute error of 0.0820 ppm and a standard deviation of 0.0756 ppm .



Fig. 4.1.: In the middle of the picture is the OpenSense testbox above the white power box. In the background are various NABEL sensor air inlets, which suck ambient air into the measurement station.

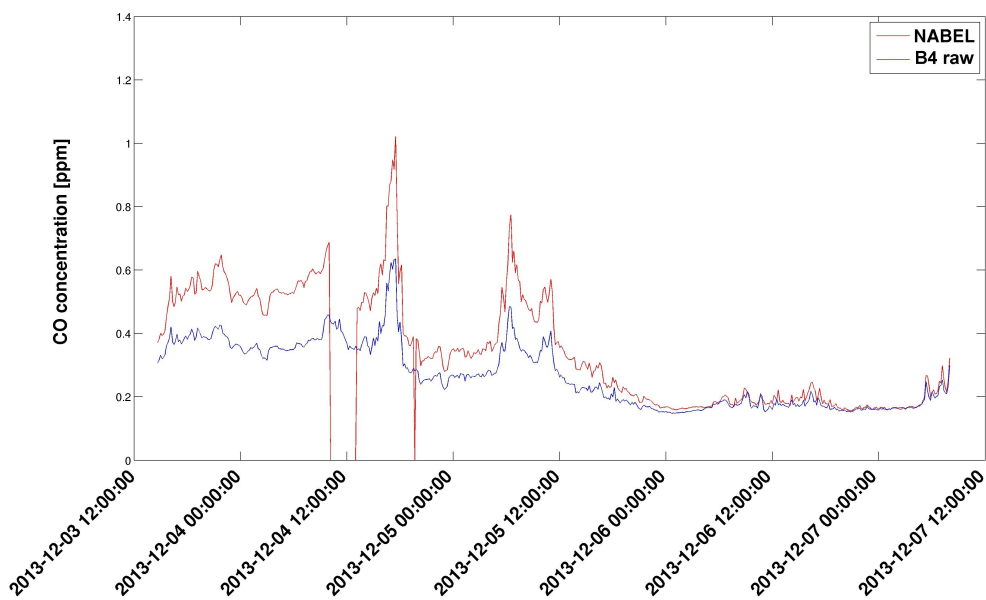


Fig. 4.2.: CO: B4 and NABEL readings over time, aggregated over 10 minutes

It also shows that the CO concentration is higher during the day than in the night, like on the 6th December 2013. This can be traced back to the fact that the two main CO sources, traffic and industrial factories, are more active during the day.

Calibration

In order to lessen the average absolute error, the B4 sensor can be calibrated based on the NABEL values. This can be done by deriving a calibration curve, which shows the relation between the B4 and NABEL values, plotted in Fig. 4.3. The calibration curve is found by

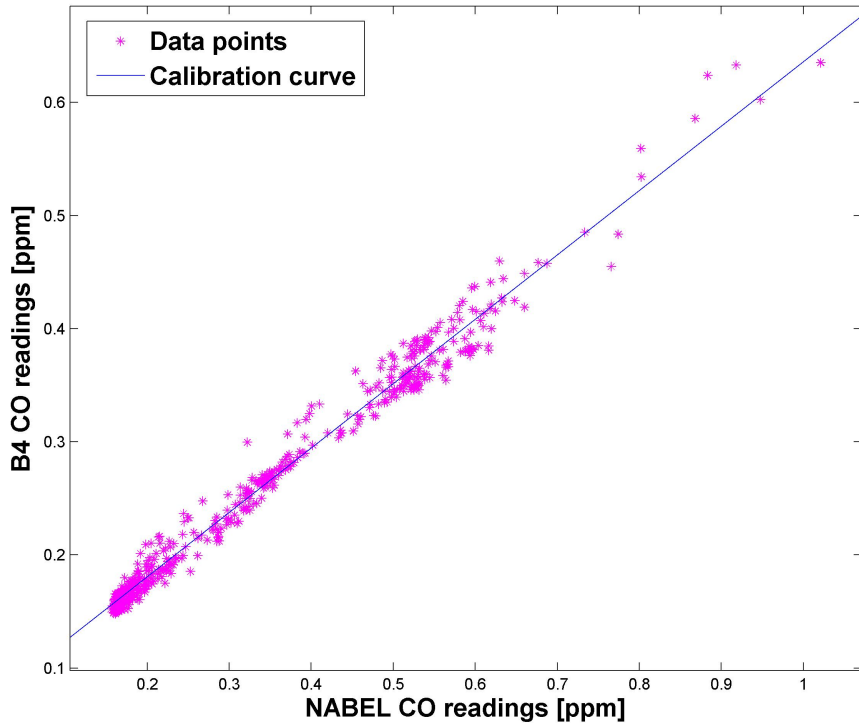


Fig. 4.3.: CO: NABEL vs. B4 readings and calibration curve

fitting a polynomial with degree 1 into the datapoints. The employed interpolation is a least square approach.

This curve can now be applied to the previous B4 values: If $f : y = f(x)$ describes the function of the calibration curve, and y are the B4 and x the NABEL values, then the calibrated B4 values can be found by

$$x_{cal} = f^{-1}(x)$$

The calibrated data is shown in Fig. 4.4. The metrics improved significantly, the absolute error lies now in the range of $[10^{-5}, 0.096]$ ppm with an average absolute error of just 0.0168 ppm and a standard deviation of 0.0151 ppm.

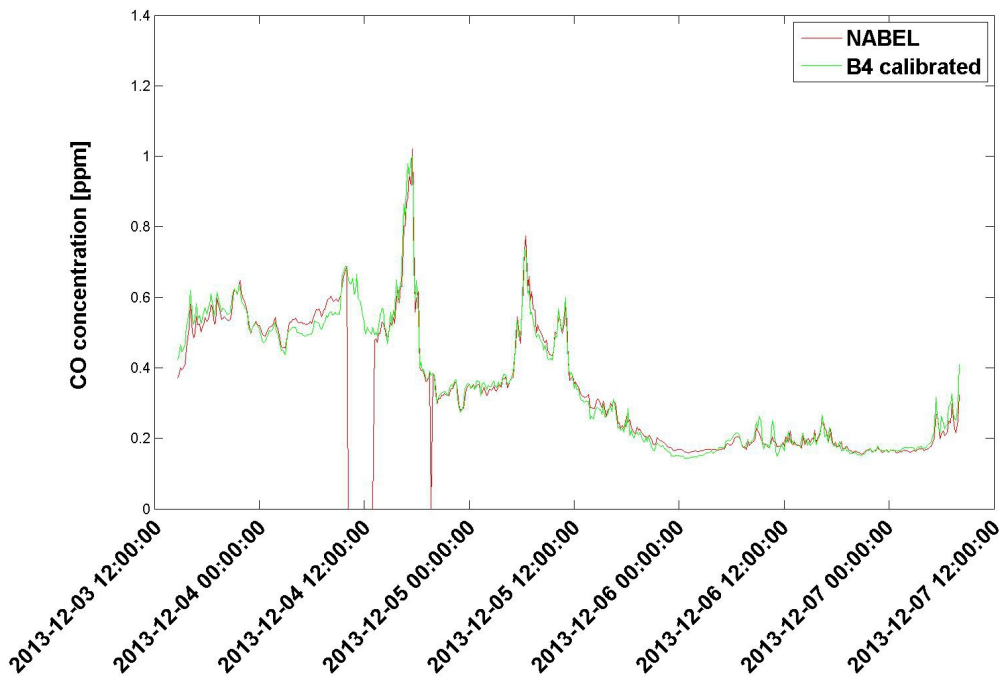


Fig. 4.4.: CO: Calibrated B4 and NABEL readings over time

4.1.2. Carbon Monoxide With Auxiliary Electrode Influence

As mentioned in Chapter 2.2 the auxiliary electrode can be used for signal correction, by subtracting the AUX values from the WE ones at every sample. The AUX voltages for the dataset which has been used in the previous section are plotted in Fig. 4.5.

The average AUX output equals 10.38mV, which corresponds to a CO concentration of 0.049ppm. However due to a very noisy signal and the fact that B4 values are in general smaller than the NABEL ones, the effect on the overall result is neglectable.

The influence of the AUX electrode actually causes slightly worse metrics compared to the basic case. The average absolute error is 0.0172 ppm with a standard deviation of 0.0164 ppm in a range of $[3 * 10^{-5}, 0.1301]$ ppm.

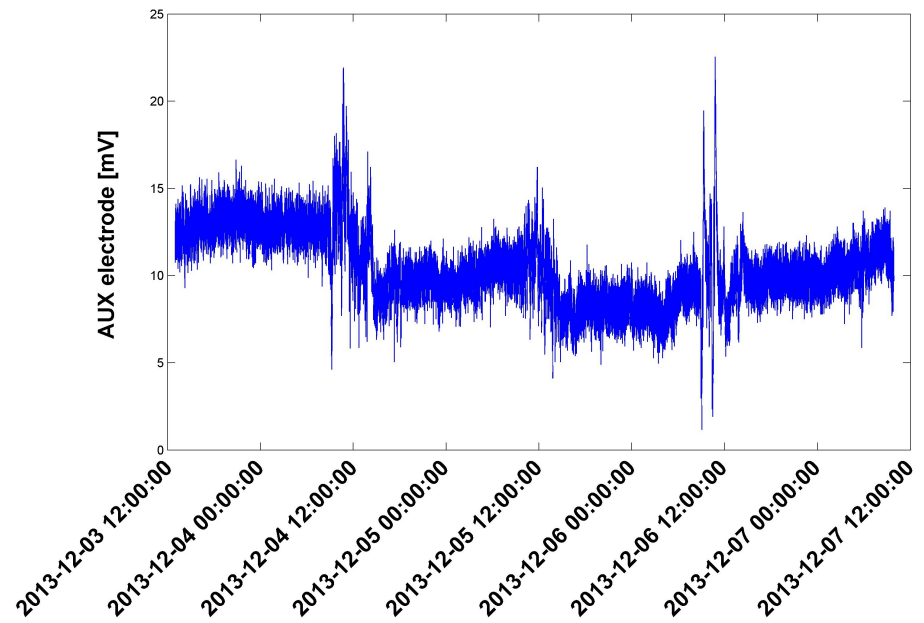


Fig. 4.5.: AUX values [mV] for the CO sensor for readings every 10 seconds

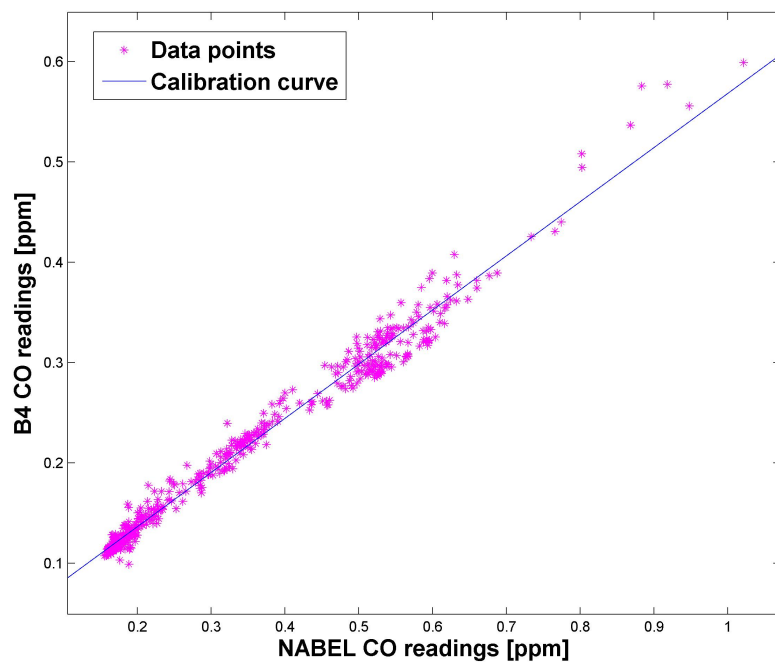


Fig. 4.6.: CO: NABEL vs. B4 readings and calibration curve after AUX correction

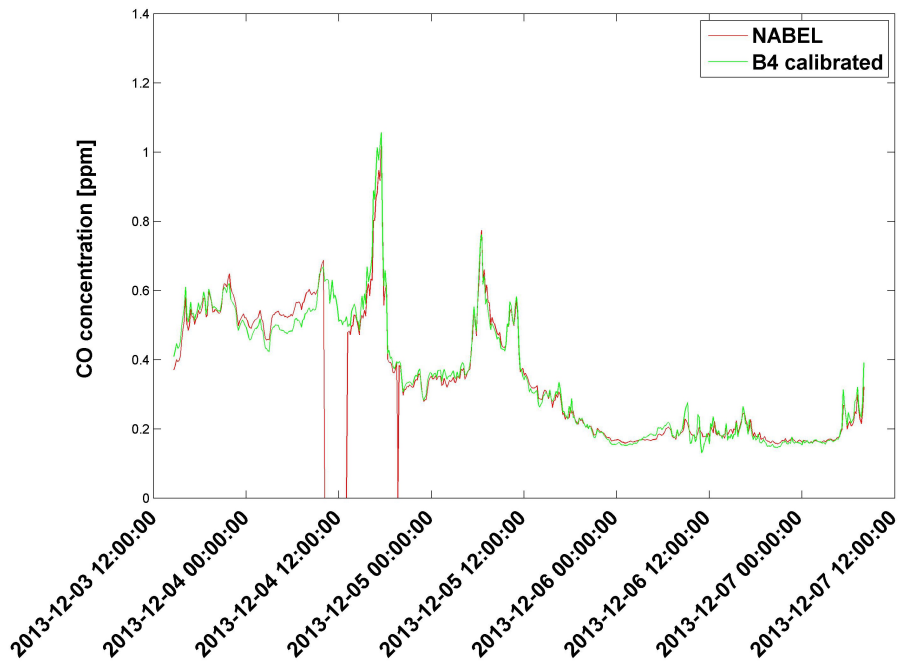


Fig. 4.7.: CO: Calibrated B4 and NABEL readings over time after AUX correction

Hence it could not be shown that the impact of the AUX electrode can be used to improve the sensor performance, however it does not disprove its purpose as the outcome might improve with different environmental conditions.

4.1.3. Nitrogen Dioxide

Over the same time period the OpenSense measurement box also collected NO_2 data, which is evaluated in the same manner as CO .

Raw Data

Fig. 4.8 shows the sensor readings over a similar time period. Usually the B4 sensor correlates to the NABEL sensor, like for the CO sensor in the previous section. However the NO_2 sensor shows for certain time periods a behaviour which does not correlate to the NABEL readings, e.g. between 5th December 2013 13:00:00 CET and 7th December 2013 11:00:00 CET.

The reason for this behaviour is the sensor's cross-sensitivity to interfering gases, especially to ozone (O_3). The cyan curve in Fig. 4.8 shows the O_3 level in ppb for the same time period. It can be seen that

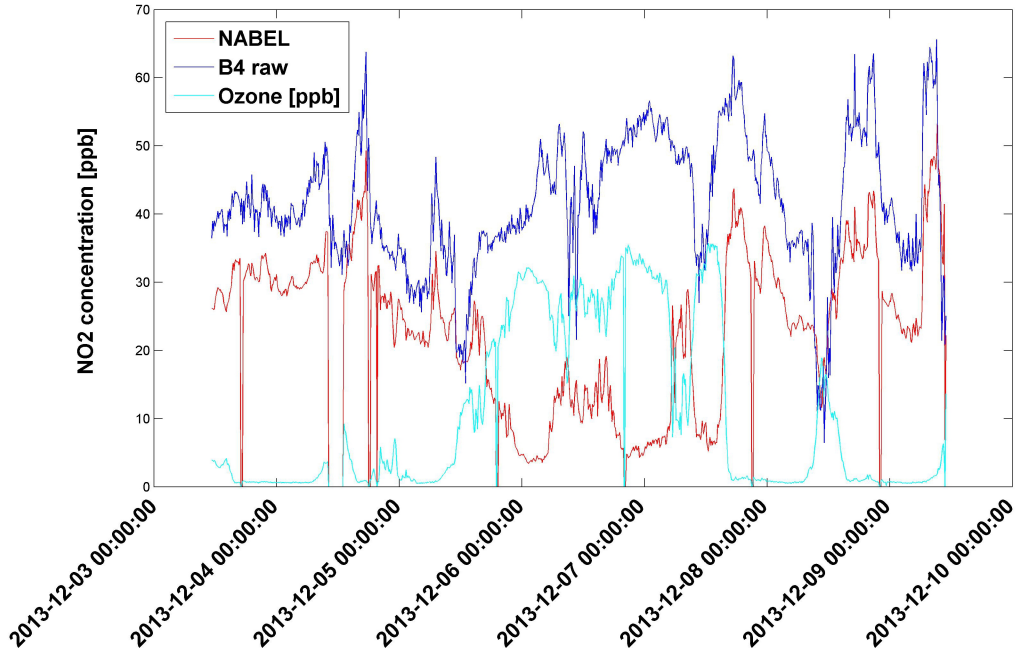


Fig. 4.8.: NO_2 : NABEL, B4 and Ozone (O_3) readings over time, aggregated every 10 minutes

the O_3 concentration was remarkably high between 5th December 2013 13:00:00 CET and 7th December 2013 11:00:00 CET, even further the B4 correlates more with O_3 than with the NABEL readings. According to the datasheet the maximum cross-sensitivity of the sensor for O_3 is 70% at 100 ppb O_3 , whereas it is only 0.1% for 10 ppm CO. [7]

Calibration

A meaningful calibration curve for a dataset which includes these high O_3 concentration sections cannot be found and would actually worsen the accuracy of the calibrated data. In order to review the NO_2 sensor performance only data sections were considered where O_3 does not exceed an upper limit of 3 ppb.

The calibration curve is shown in Fig. 4.9 and the resulting calibrated data in Fig. 4.10. Fig. 4.11 shows only the data which has been calibrated. Again it was possible to lessen the average absolute error significantly. Before calibration the average absolute error was 12.03 ppb with a standard deviation of 3.767 ppb in the range of [0.625, 23.48] ppb. With applying the calibration curve from Fig. 4.9 the metrics improve to an average absolute error of 2.178 ppb with a standard deviation of 1.880 ppb in the range of $[3 * 10^{-3}, 15.30]$ ppb.

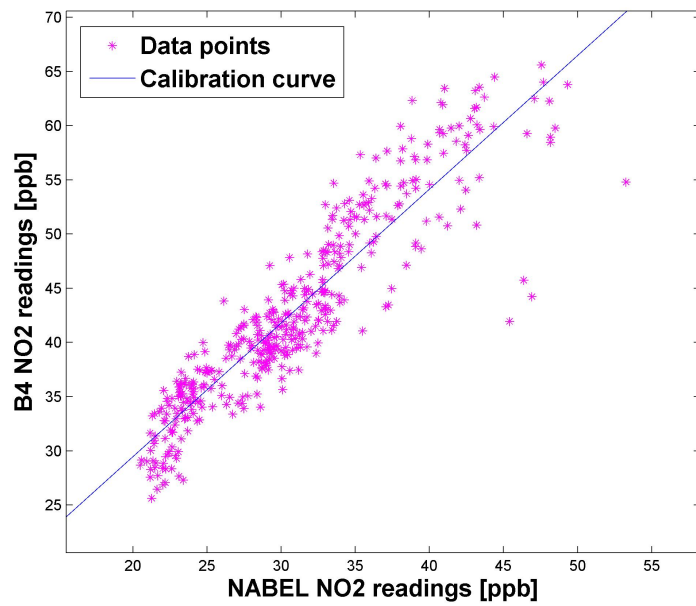


Fig. 4.9.: NO₂: NABEL vs. B4 readings and calibration curve

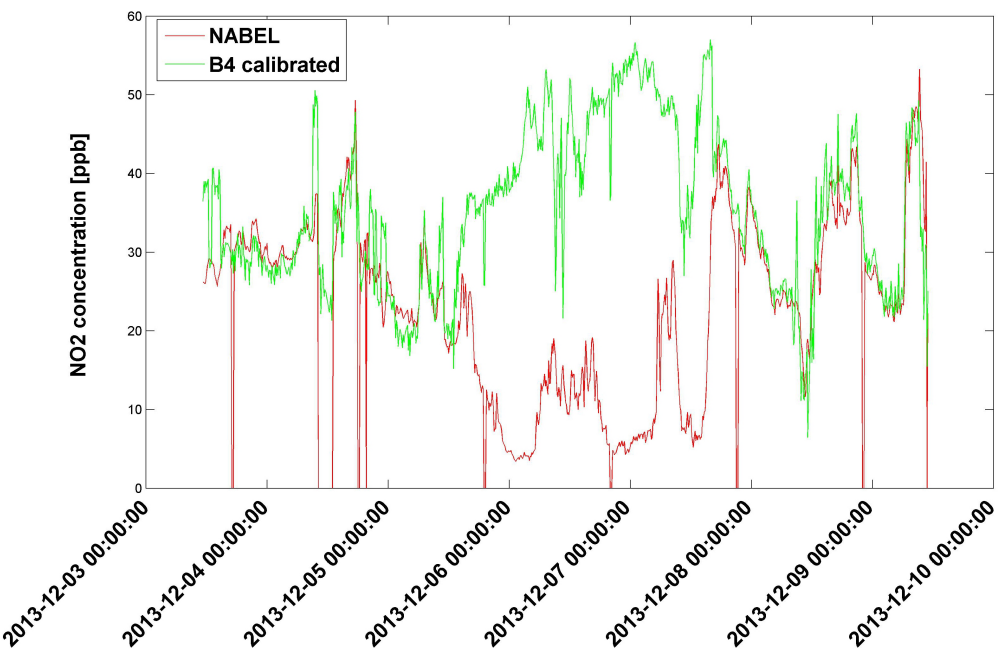


Fig. 4.10.: NO₂: Calibrated B4 and NABEL readings over time

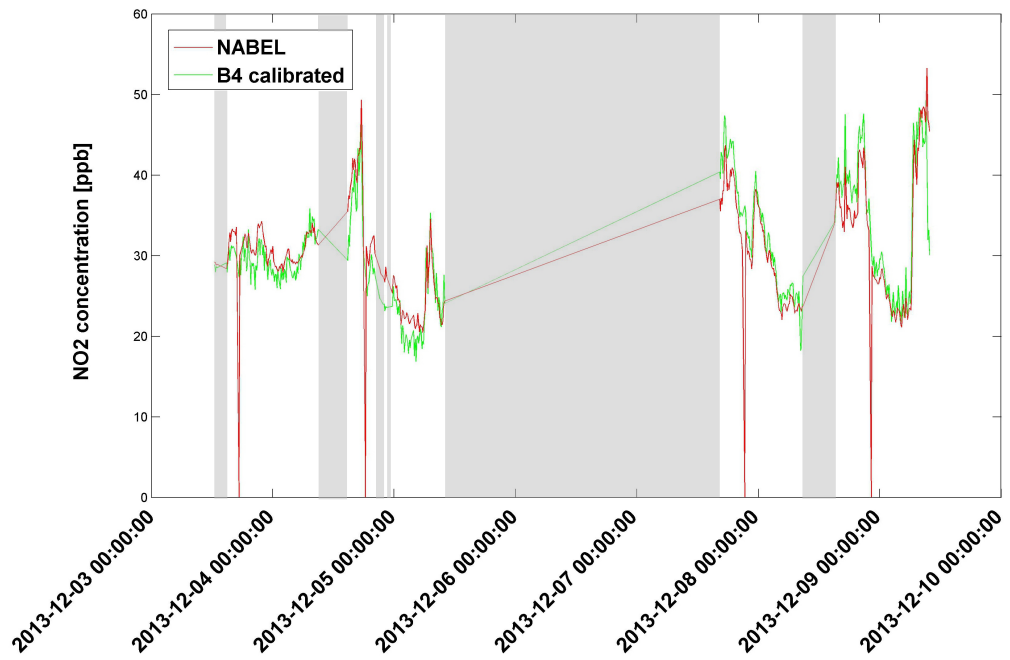


Fig. 4.11.: NO₂: Calibrated B4 and NABEL readings, grey areas denote the periods where the O₃ concentration was over 3ppb

4.2. Overall Results

The B4 sensor performance evaluation based on the highly reliable and accurate dataset provided by NABEL showed that the B4 sensors correlate very well with the NABEL measurements. In general, the data shows an offset which can be significantly reduced by using a simple calibration technique.

However, it was not possible to show the purpose of the AUX electrode for the CO sensor. The possibility of a benefit needs further attention, e.g. testing under different environmental conditions.

Further the results of the NO_2 pointed out the cross sensitivity of such low-cost gas sensors. The NO_2 B4 sensor is extremely sensitive to the presence of O_3 which made it impossible to use the data for calibration during a time with a high O_3 concentrations.

Overall the important metrics for all sensors are summarized in Tables 4.1, 4.2 and 4.3

CO	Uncalibrated	Calibrated
Average absolute error	0.0820 ppm	0.0168 ppm
Standard deviation	0.0756 ppm	0.0151 ppm
Range	$[10^{-4}, 0.38]$ ppm	$[10^{-5}, 0.096]$ ppm

Tab. 4.1.: CO sensor performance metrics

CO-AUX	Uncalibrated	Calibrated
Average absolute error	0.1306 ppm	0.0172 ppm
Standard deviation	0.0808 ppm	0.0164 ppm
Range	$[0.028, 0.442]$ ppm	$[3 * 10^{-5}, 0.130]$ ppm

Tab. 4.2.: CO-AUX sensor performance metrics

NO_2	Uncalibrated	Calibrated
Average absolute error	12.03 ppb	2.178 ppb
Standard deviation	3.767 ppb	1.880 ppb
Range	$[0.625, 23.48]$ ppb	$[3 * 10^{-3}, 15.3]$ ppb

Tab. 4.3.: NO_2 sensor performance metrics

Conclusions and Future Work

This work presented the integration of two gas sensors, carbon monoxide (CO) and nitrogen dioxide (NO_2) of the Alphasense B4 series, into the OpenSense sensor box. On the hardware side two fundamental decisions had to be made. First an appropriate choice for the power supply. Due to the sensor's low power consumption and the need for a low-noise input voltage the final decision came to a low-dropout voltage regulator (LDO) from STMicroelectronics. It outperforms many other models in the same category in terms of accuracy and output noise.

The second choice was the handling of the analog-digital signal conversion. A careful examination of the sensor specifications (e.g. sensitivity and resolution) showed that the ADC on the OpenSense sensor box baseboard meets the demands. The ADC has a resolution of 16Bits and can handle a maximum of 10 channels. Three of these channels are free and available to measure one sensor's working and auxiliary electrodes and a second sensor's working electrode.

On the software side a new plugin was added to the backlog software, which is responsible for periodically reading out the sensor signals and store them in the local database. In an additional step the data is transferred to the OpenSense back-end server, which is running the Global Sensor Network (GSN). This was done by creating a wrapper, which is streaming the data from the sensor box to a virtual sensor, the main component in GSN.

The work concludes with a performance evaluation and discussion of the results of the presented solution. The B4 sensor data was compared to a static measurement station in Dübendorf (ZH) operated by NABEL. Data was collected by placing the sensor box next to the NABEL sensors for multiple days. The results show that the B4 sensor's signals have an offset when compared to the NABEL data. The offset of the CO sensor could be reduced by applying a simple calibration curve. In the end, the average absolute error could be decreased from 82 ppb to 16.8 ppb which is about 8.4% of the minimal CO signal that has been measured. Yet it was not possible to show that the influence of the auxiliary diode is improving the sensor performance, which might be the case under other testing conditions.

The NO_2 data is also showing an offset compared to the NABEL data but suffers from the sensor's cross-sensitivity to ozone (O_3). During

time periods where the O_3 concentration was high the sensor signal was not correlating to the NABEL NO_2 signals but rather to the O_3 sensor readings. This made it impossible to find a meaningful calibration curve during this time periods. Therefore the evaluation is only based on the data where the O_3 concentration is below 3 ppb. With the same calibration technique it was again possible to decrease the average absolute error from 12 ppb to 2.2 ppb, which is about 11% of the smallest NO_2 value that has been measured.

In conclusion the work shows that it is possible with the right choice of hardware components and a simple calibration technique to get a good performance with the used low-cost gas sensors. The results support the future appliance of the Alphasense B4 sensor for urban air pollution monitoring in mobile sensor nodes.

In future, different aspects of the system can be extended:

- The evaluation of the NO_2 sensor showed that such low-cost gas sensors are sensitive to interfering gases, like O_3 for the NO_2 sensor. Further testing might show additional interference problems under different conditions, e.g. temperature and humidity. Therefore, the performance evaluation is not complete and should be extended with data for example gathered during warm and humid summer days.
- The influence of the AUX electrode needs further examination as well.
- It was not possible to find a calibration curve for NO_2 during high O_3 concentration periods and therefore this data was not considered. The chosen upper limit of 3 ppb is extremely low and the average O_3 concentration for example during summer might be notably higher. Hence, the O_3 interference should also be considered for sensor calibration, this can be done e.g. by finding a calibration curve based on two variables: B4 vs. NABEL and O_3 .
- In Chapter 2.5.3 the idea of a Faraday cage around the sensor and its electronics were presented but not implemented in the final design. This can be done and to test whether it improves the sensor performance.

Bibliography

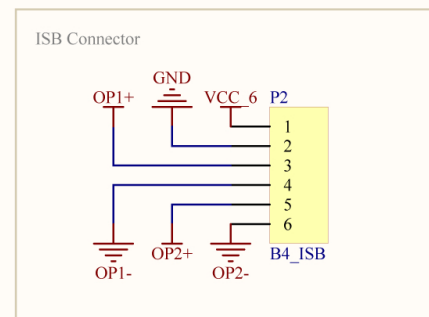
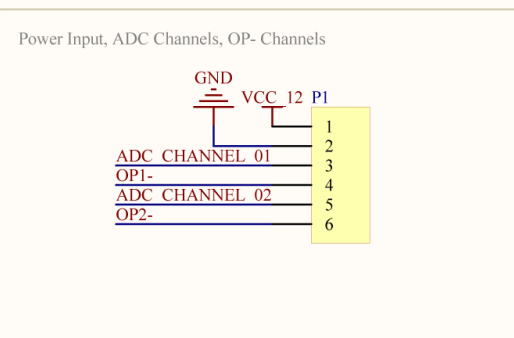
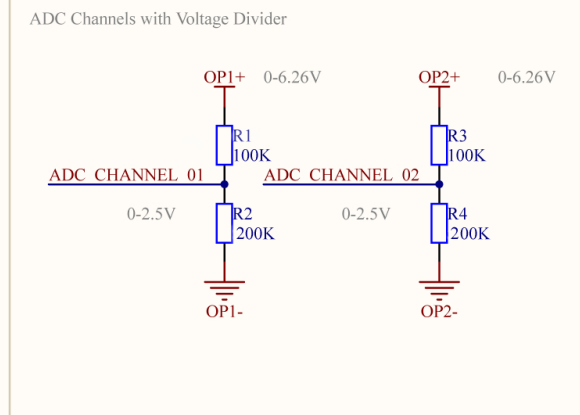
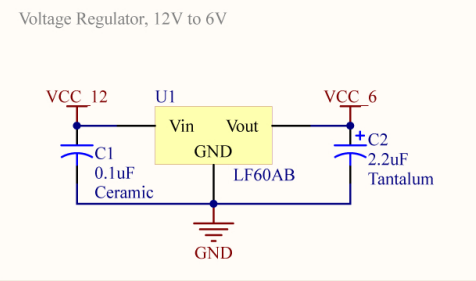
- [1] Matter Aerosol. *MiniDiSC*. Datasheet.
- [2] Alphasense. *4 to 20 mA Digital Transmitter Board Alphasense Type A and B Toxic Gas Sensors*. Datasheet.
- [3] Alphasense. *AAN 104, How Electrochemical Gas Sensors Work*. Application Note.
- [4] Alphasense. *CO-AF Carbon Monoxide Sensor*. Datasheet.
- [5] Alphasense. *CO-B4 Carbon Monoxide Sensor, 4-Electrode*. Datasheet.
- [6] Alphasense. *NO2-A1 Nitrogen Dioxide Sensor*. Datasheet.
- [7] Alphasense. *NO2-B4 Nitrogen Dioxide Sensor, 4-electrode*. Datasheet.
- [8] Analog Devices. *AD7708/AD7718, 8-/10-Channel, Low Voltage, Low Power, $\Sigma - \Delta$ ADCs*. Datasheet.
- [9] Texas Instruments. *uA78M00 SERIES, POSITIVE-VOLTAGE REGULATORS*. Datasheet.
- [10] Opensense project website. <http://www.opensense.ethz.ch/>, December 2013.
- [11] SGX Sensortech. *MiCS-OZ-47 Ozone Sensing Head with Smart Transmitter PCB*. Datasheet.
- [12] STMicroelectronics. *LFxxAB, LFxxC, Very low drop voltage regulators with inhibit*. Datasheet.
- [13] GSN Team. *Global Sensor Network*. Documentation.
- [14] NABEL website. http://www.empa.ch/plugin/template/empa/699/*/-l=1, December 2013.

A

Appendix

A.1. Hardware

A.1.1. Schematics



Eidgenössische Technische Hochschule Zürich
Swiss Federal Institute of Technology Zurich

Zeichnungs Titel:

OpenseNSE - Alphasense B4

Zeichnungsnr.: * Rev: 1.0

Datum: 10.10.2013 17:03:42

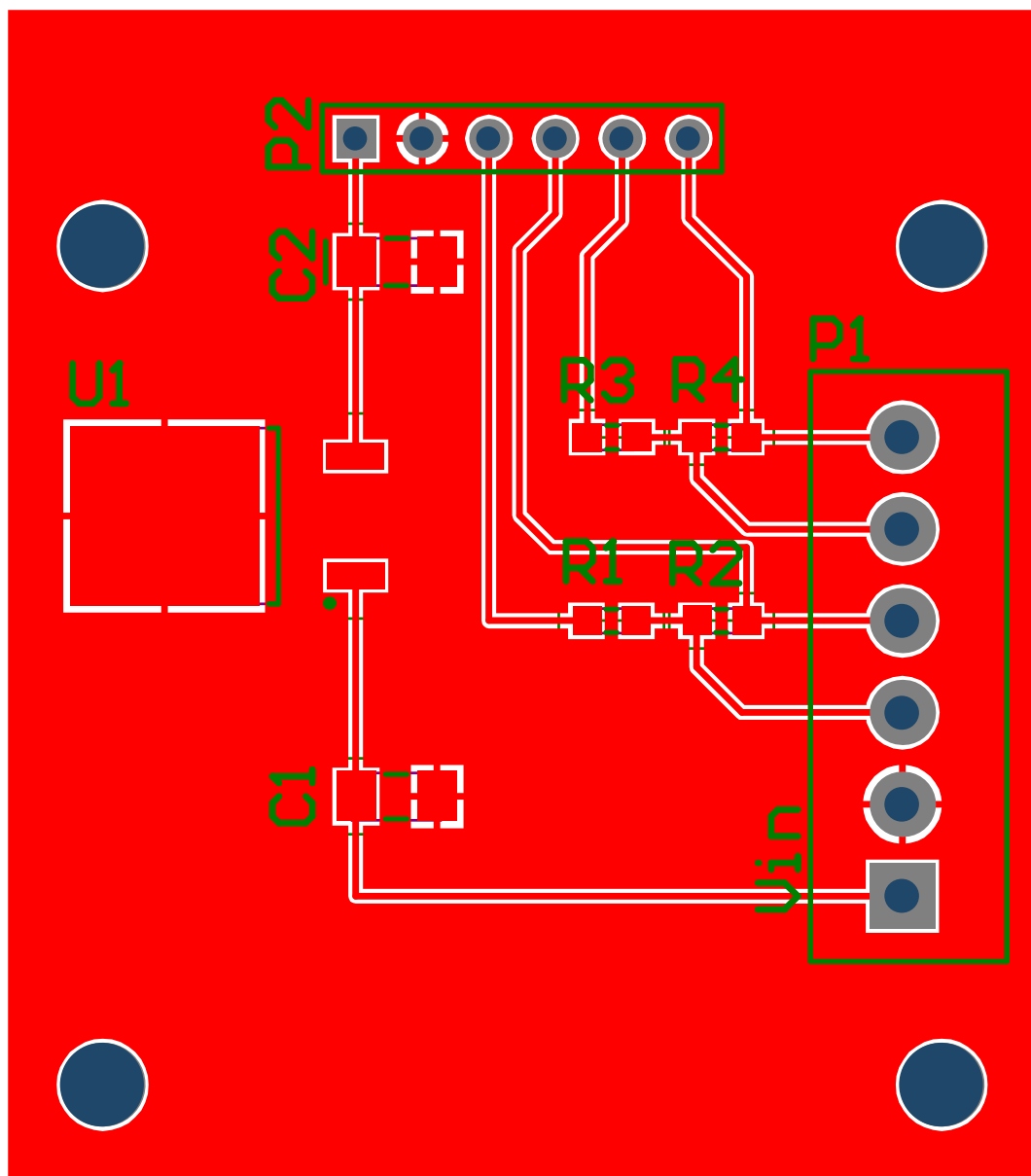
Format: Institut: ETH Zurich, Institut TIK, Group TEC Projekt: openseNSE_alphasense_b4.SchDoc

A4 Q Ersteller: Balz Maag <bmaag@student.ethz.ch>

Seite 1 von 1

File: C:\Users\Balz\Documents\svn\projects\0012_openseNSE\0001_alphasense_b4\rev1.0\openseNSE_alphasense_b4.SchDoc







A.1.2. Components list

The components list for the PCB is shown in Table A.1.

Name	Value/Part No.	Size/Package	Manufacturer
R1, R3	100kΩ	0603	-
R2, R4	200kΩ	0603	-
U1	LF60AB	DPAK	STMicroelectronics
C1	0.1μF ceramic	1206	-
C2	2.2μF tantalum	1206(Type A)	-
P2	Compona 248 214-0	6x1	Compona
P1	SL 3.50/90G	6x1 or two 3x1	Weidmuller

Tab. A.1.: List of components

A.1.3. Baseboard Changes

The sensor needs to be connected to the baseboard using two different connectors. The power is available on P20 (baseboard v2). The ADC channels are connected to P13, however for correct operation some changes on the baseboard need to be made. The changes are shown in Table A.2.

baseboard v2 rev1.0			baseboard v2 rev2.0		
Part	Old Value	New Value	Part	Old Value	New Value
R138	100Ω	0Ω	R138	100Ω	0Ω
R139	100Ω	0Ω	R139	100Ω	0Ω
R140	100Ω	0Ω	R140	100Ω	0Ω
R82	100kΩ	0Ω	R82	100kΩ	0Ω
R83	10kΩ	100kΩ	R83	15kΩ	100kΩ
R84	100kΩ	0Ω	R84	100kΩ	0Ω
R85	15kΩ	100kΩ	R85	15kΩ	100kΩ
D26	-	remove	R14	100kΩ	0Ω
D27	-	remove	R101	15kΩ	100kΩ
D28	-	remove	D26	-	remove
			D27	-	remove
			D28	-	remove

Tab. A.2.: Required changes to baseboard v2 rev1.0 and rev2.0

A.2. Software

A.2.1. Backlog Configuration

In the file *backlog.cfg* under the section [*B4SensorPlugin_options*] different parameters for the B4SensorPlugin can be set, see the description in Table A.3. These parameters will be read during the initialization phase of the plugin.

In the file *BackLogMessage.py* a unique message identifier number for the B4SensorPlugin has to be defined, it is set to `B4SensorPlugin = 115`.

Parameter	Description	Default
priority	Specifies the order messages are send to GSN	10
backlog	True/false: activates plugin in backlog	true
gps_device	GPS device location	/dev/acm/ublox6
gps_data	True/false: adds gps data to the sensor reading	true
poll_interval	Interval in seconds the plugin is executed	10
ain1	Location of proc file for ADC channel 1	/proc/ad77x8/ain1
ain2	Location of proc file for ADC channel 2	/proc/ad77x8/ain2
ain3	Location of proc file for ADC channel 3	/proc/ad77x8/ain3
adc_config_path	Location of proc file for ADC config file	/proc/ad77x8/config
adc_config_flag	True/false: activates ADC configuration	false
dual_sensor	True/false: true = read two sensors, false = read one sensor	true
we_zero_mV_01	Working electrode offset for sensor 1 [mV]	292 (for CO)
aux_zero_mV_01	Auxiliary electrode offset sensor 1 [mV]	320 (for CO)
sensitivity_nA_01	Sensitivity for sensor 1 [nA]	653 (for CO)
we_zero_mV_02	Working electrode offset for sensor 2 [mV]	226 (for NO ₂)
aux_zero_mV_02	Auxiliary electrode offset sensor 2 [mV]	223 (for NO ₂)
sensitivity_nA_02	Sensitivity for sensor 2 [nA]	-486 (for NO ₂)
gain_01	ISB buffer gain for CO, H ₂ S, SO ₂ , NO [nA/mV]	0.8
gain_02	ISB buffer gain for NO ₂ [nA/mV]	0.726
gain_03	ISB buffer gain for O ₃ [nA/mV]	0.746
Rgnd	Rgnd resistor value for voltage divider [kOhm]	66.6
Rvin	Rvcc resistor value for voltage divider [kOhm]	100

Tab. A.3.: B4SensorPlugin.py parameters in *backlog.cfg*

List of Tables

2.1.	LF60AB specifications	8
2.2.	Sensor and ISB specifications	9
2.3.	AD7708 specifications	10
2.4.	Sensor/ISB specifications after voltage level shift by factor 0.399	11
3.1.	ADC configuration options	18
3.2.	Different data package formats	21
4.1.	CO sensor performance metrics	34
4.2.	CO-AUX sensor performance metrics	34
4.3.	NO ₂ sensor performance metrics	34
A.1.	List of components	44
A.2.	Required changes to baseboard v2 rev1.0 and rev2.0	44
A.3.	B4SensorPlugin.py parameters in <i>backlog.cfg</i>	46

List of Figures

1.1.	Ultrafine particle distribution in Zürich in the fall of 2013 [10]	2
1.2.	Sensor box on a VBZ Cobra-tram [10]	3
2.1.	Coarse overview of hardware components	5
2.2.	LDO with decoupling capacitors	8
2.3.	Voltage divider circuit	10
2.4.	Decoupled LF60AB circuit	12
2.5.	Voltage divider circuits and ADC channel inputs	12
2.6.	ISB Connector	13
2.7.	Power input and ADC channels	13
2.8.	PCB layout	14
2.9.	Stacked PCBs and the B4 sensor head	14
2.10.	Exterior wall of the OpenSense measurement box, left: B4 sensor head, right: sensor cover	15
2.11.	OpenSense measurement box with two B4 sensors to monitor CO and NO ₂ concentrations	15
3.1.	Coarse overview of the different software parts	17
3.2.	B4 plugin basic flowchart	19
3.3.	Virtual sensor data from 7 th December 2013 at 14:21:21.986 CET	23
3.4.	CO [ppm] data on the 7 th December 2013 between 00:47 and 08:45 CET	23
4.1.	In the middle of the picture is the OpenSense testbox above the white power box. In the background are various NABEL sensor air inlets, which suck ambient air into the measurement station.	26
4.2.	CO: B4 and NABEL readings over time, aggregated over 10 minutes	26
4.3.	CO: NABEL vs. B4 readings and calibration curve	27
4.4.	CO: Calibrated B4 and NABEL readings over time	28
4.5.	AUX values [mV] for the CO sensor for readings every 10 seconds	29

4.6. CO: NABEL vs. B4 readings and calibration curve after AUX correction	29
4.7. CO: Calibrated B4 and NABEL readings over time after AUX correction	30
4.8. NO ₂ : NABEL, B4 and Ozone (O_3) readings over time, aggregated every 10 minutes	31
4.9. NO ₂ : NABEL vs. B4 readings and calibration curve	32
4.10. NO ₂ : Calibrated B4 and NABEL readings over time	32
4.11. NO ₂ : Calibrated B4 and NABEL readings, grey areas denote the periods where the O_3 concentration was over 3ppb	33